Ion-Ion De-Association and Association of Strong Electrolytes at High Dilution from Nuclear Magnetic Relaxation Measurements

E. Detscher, H. G. Hertz, M. Holz, and Xi-an Mao*

Institut für Physikalische Chemie und Electrochemie der Universität Karlsruhe, D-76128 Karlsruhe

Z. Naturforsch. **50a**, 487–501 (1995); received January 28, 1995

Dedicated to Professor E. Wicke on the occasion of his 80th birthday

Proton magnetic relaxation rates in the system $N(CH)_3)_4Br/NiBr_2/D_2O$, $N(CH_3)_4Br/MnBr_2/D_2O$, $Ni(OOCCH_3)_2/D_2O$ and $Mn(OOCCH_3)_2/D_2O$ have been measured as a function of the solute concentration in the range $0.002 < c^* \lesssim 1$ m. Division by the concentration c^* and by a quantity characterizing the ionic motion yields the association parameter (A-parameter). A decreases and increases with decreasing concentration for the systems involving cation-cation and cation-anion interaction, respectively. The relaxation rates of $^{35}Cl^-$, $^{133}Cs^+$, and $^{25}Mg^{++}$ in diamagnetic aqueous solutions have also been measured down to high dilution. Here as well in most cases we have found an increase of the A-parameter with decreasing salt concentration, indicating ion-ion association at high dilution. A comparison with the results of the Debye-Hückel theory is given; there is qualitative agreement. Our experimental results for $^{35}Cl^-$ generally do not support theoretical considerations in the literature, where a $Cl^- - Cl^-$ association was postulated.

1. Introduction

In the galvanic cell the reversible electric work to be supplied to the system when a chemical reaction $\nu_+ A + \nu_- B \Rightarrow A_{\nu+} B_{\nu-}$ is proceeding is given by an appropriate standard value plus a certain contribution which is due to the entropy variation and an additional composition dependence of the total Gibbs free energy. At high dilution of the solute $A_{\nu+}B_{\nu-}$, the latter contribution is due to the electrostatic interaction between the ions. Thus, when a given ion, cation or anion, enters into the solution, it takes on a state of potential energy caused by the surrounding other ions. Moreover at high dilution the contributions of cations and anions are determined by the Debye-Hückel ion-ion distribution functions $g_{+-}(r)$, $g_{++}(r)$ and $g_{--}(r)$, and for electrolyte concentration $c \to 0$ the corresponding expression for the electric work contains a term

$$-RT\text{const}\sqrt{I} = -RT\text{const}[\tfrac{1}{2}(z_+^2 c_+ + z_-^2 c_-)]^{\frac{1}{2}}, \quad (1)$$

where I is the ionic strength. As is well known, other properties show the $\sqrt{c}$-dependence as well.

Electrolytes for which (1) holds are called "strong electrolytes". Strong electrolytes are considered to be completely dissociated at high dilution. But this statement is inaccurate because it is not based on a precise definition of the term "completely dissociated". The generally used, loose understanding of the expression "completely dissociated" is based on the fact that the radius of the sphere around the central ion containing on its surface the total charge of all other ions increases more and more as the concentration of the electrolyte decreases. But this argument contains two conceptual objects or steps, the ion-ion pair distribution functions ($+-$ and $++$, $--$) and the interpretation of what is essentially the difference of the corresponding local densities times r^2. In fact, the anion-cation pair distribution function contracts as the electrolyte concentration decreases, under dilution the cation is more strongly attracted by the anion and vice versa and when compared with associating non-electrolyte solutions (see e.g. [1–3]) this effect must be called association. Thus in strong electrolyte solution we have cation-anion association as the solution is diluted, an elementary fact which, surprisingly enough, is generally not known. Correspondingly repulsion of ions of equal charge gives de-association.

All experimental methods so far used to study radial distribution functions break down if the atoms of interest are as highly diluted as is the case here. So the results to be presented here are – apart from [1] – the first experimental proof of the pertinent properties of ion-ion distribution functions, association, and in con-

* On leave from: Laboratory of Magnetic Resonance, The Chinese Academy of Sciences, Wuhan 430071, China.

Reprint requests to Prof. Dr. H. G. Hertz.

0932-0784 / 95 / 0400-0487 $ 06.00 © – Verlag der Zeitschrift für Naturforschung, D-72027 Tübingen

trast to that, de-association at high dilution, and thereby, as will be shown below, the Debye-Hückel distribution functions (see also lit. ref. in [4]).

Reformulating our above statement slightly, we can also say that the cation-anion distribution function, $g_{+-}(r)$, has the property that with increasing dilution of the electrolyte the ratio of the local to the mean counter-ion concentration increases which represents association [1], i.e.

$$\frac{\mathrm{d}n^*_{+-}}{\mathrm{d}c} \equiv \frac{\mathrm{d}}{\mathrm{d}c} 4\pi \int_a^{r^*} \left(\frac{a}{r}\right)^6 g_{+-}(r) r^2 \,\mathrm{d}r < 0 \,. \tag{2}$$

Here the term local refers to a region around the reference ion given by a radius r^* with $(a/r^*)^6 \approx 1/10$, where a is the closest distance of approach between cations and anions. The quantity n^*_{+-} we call the reduced first coordination number, $n^*_{+-} = n_{+-}/c$, where n_{+-} is the first coordination number defined by the cut-off function $(a/r)^6$ of a cation with respect to the counter anions.

n^*_{+-} appears in the expression for the intermolecular nuclear magnetic relaxation rate $(1/T_1)_{\text{inter}}$, if the corresponding relaxation mechanism is based on nuclear magnetic dipole-dipole interaction between cations and anions [1, 4]:

$$\left(\frac{1}{T_1}\right)_{\text{inter}} = K c \tau n^*_{+-} \,, \tag{3}$$

where the constant K contains nuclear and ionic properties and τ is an appropriate (microscopic) correlation time. In those cases where τ depends on r, the form of (3) implies that a proper approximation for τ is chosen (see below). The $1/r^6 = (1/r^3)^2$ dependence is due to the fact that (3) represents the mean squared magnetic dipole-dipole interaction, multiplied by a correlation time.

For one $1-1$ electrolyte, namely $N(CH_3)_4F$, it has indeed been shown that the relation (2) is valid. With decreasing salt concentration c the quantity

$$A \equiv \frac{(1/T_1)_{\text{inter}}}{c\tau} = K n^*_{+-} \tag{4}$$

increases; thus we have $\mathrm{d}n^*_{+-}/\mathrm{d}c < 0$ in agreement with the Debye-Hückel theory (see below). In this experiment the ^{19}F relaxation rate of $N(CH_3)_4F$ in D_2O was measured [1].

When we now consider the like ion distribution, it is expected that e.g. the ratio of the local cation to mean cation concentration around a reference cation decreases with decreasing salt concentration, which is de-association, i.e.

$$\frac{\mathrm{d}n^*_{++}}{\mathrm{d}c} = \frac{\mathrm{d}}{\mathrm{d}c} 4\pi \int_a^{r^*} \left(\frac{a}{r}\right)^6 g_{++}(r) r^2 \,\mathrm{d}r > 0$$

and also (5)

$$\frac{\mathrm{d}n^*_{--}}{\mathrm{d}c} = \frac{\mathrm{d}}{\mathrm{d}c} 4\pi \int_a^{r^*} \left(\frac{a}{r}\right)^6 g_{--}(r) r^2 \,\mathrm{d}r > 0 \,.$$

This expectation comes from the fact that ions of equal charge repel one another and that at high concentration the solution of noble gas ions due to screening of the charges looks more and more like a solution of rigid spheres. The relation (5) describes a flattening of the ion-ion distribution functions, whereas (2) describes a sharpening of $g_{+-}(r)$ with decreasing concentration. The relations (5) follow from the Debye-Hückel theory as well, as will be shown below. The validity of this relations, that is of

$$\frac{\mathrm{d}}{\mathrm{d}c}\left(\frac{(1/T_1)_{\text{inter}}}{c\tau}\right) = \frac{\mathrm{d}}{\mathrm{d}c} K n^*_{++} > 0 \,, \tag{6}$$

has not yet been demonstrated experimentally, and this proof will be one of the objects of the present investigation. In order to make the constant K sufficiently large in the present study, we employed the magnetic dipole-dipole interaction with a paramagnetic ion, so we are reporting on ^1H relaxation time measurements of the systems $N(CH_3)_4Br/NiBr_2/D_2O$ and $N(CH_3)_4Br/MnBr_2/D_2O$.

When paramagnetic ions act as interaction partner for the relaxing nucleus then, if the static magnetic field is properly chosen, the quantity K in (3) takes the form

$$K = \frac{(\gamma_S \gamma_I \hbar)^2 S(S+1)}{a^6} k \,, \tag{3a}$$

where γ_I nad γ_S are the gyromagnetic ratios of the proton and paramagnetic ion, respectively, S is the spin of the paramagnetic ion, $k = 4/3$ and $2/5$ for Ni^{++} and Mn^{++}, respectively. Equation (3a) holds in a range where the frequency dependence of $(1/T_1)_{\text{inter}}$ can be neglected [5–11].

Moreover, in order to check the consistency of our results we also measured the proton relaxation times of the systems $Ni(OOCCH_3)_2/D_2O$ and $Mn(OOCH_3)_2/D_2O$, so as to verify the expected property expressed as relation (2), which is valid for the cation-anion pair correlation function $g_{+-}(r)$.

Apart from ^{19}F, the ions with noble gas structure relax by nuclear quadrupole-electric field gradient interaction. This fact precludes separation of cation-anion and equal-ion relaxation effects for diamagnetic systems. But in comparison with the relaxation effects of separated cation-anion and cation-cation interaction effects it is of interest to see the combined effect of both distributions. Therefore we add some experimental results for $^{35}Cl^-$, $^{133}Cs^+$ and $^{25}Mg^{2+}$ relaxation rates in dilute aqueous solutions. The systems investigated are: HCl, LiCl, RbCl, CsCl, $MgCl_2$, CsF, CsBr, CsI, and $CsNO_3$. The underlined symbol indicates the relaxing nucleus studied.

2. Experimental

All proton T_1 measurements were performed with a Bruker SXP 4-100 pulse spectrometer combined with a Bruker electromagnet. The resonance frequency was $\nu_0 = 90$ MHz. For the T_1 measurements of the ionic nuclei ^{35}Cl ($\nu_0 = 29.39$ MHz), ^{25}Mg ($\nu_0 = 18.36$ MHz), and ^{133}Cs ($\nu_0 = 39.35$ MHz) we used a Bruker SXP pulse spectrometer combined with a Bruker Cryomagnet BZH 300/89.

T_1 values were obtained via the $180°-\tau-90°$ pulse sequence in the usual way. For weak signals occurring in highly diluted solutions we applied signal accumulation by the aid of a Bruker computer Aspect 2000.

For the proton relaxation measurements, temperature control was performed by pumping water from a thermostat through the probe head; the temperature at the position of the sample was controlled by a calibrated thermometer before and after the measurements; the temperature was $T = 25 \pm 0.3$ °C. In the cryomagnet the proton free cooling liquid Fluor Inert was pumped through the probe head, the temperature was measured in the probe head via a Pt 100 temperature control. For the very dilute $N(CH_3)_4^+$- and acetate-solutions it was necessary to remove any proton containing plastic supporting the probe coil.

All chemicals were of commercial origin, $N(CH_3)_4Br$ was dried before use during two days at 75 °C and under vacuum. Magnesium bromide was purchased as $MgBr_2 \cdot 6H_2O$. H_2O was exchanged against D_2O to a degree sufficient for our purpose (see below), the content of ^1H was controlled via high resolution NMR.

The D_2O used was usually of deuterium content 99.5 atom percent, for the proton relaxation measurements at highest dilution we had to use D_2O with 99.97% deuterium content (MSD Isotopes, Montreal, Canada). Undesired proton content of all solvents and solutions was checked by high resolution NMR. The samples were prepared by weighing. For the proton relaxation measurements in the Ni-salt solutions of high dilution it turned out that it was necessary to free the samples from oxygen by the usual freeze – thaw cycles. All samples were sealed off. The experimental error of the proton T_1 data is $\leq 2\%$, the error limit for ^{35}Cl, ^{25}Mg, and ^{133}Cs measurements is $\pm 3\%$.

3. Results

3.1 Cation-Cation Correlations

In Fig. 1 the proton magnetic relaxation rate of the mixture $N(CH_3)_4Br + NiBr_2 + D_2O$ as a function of the concentration $c^* = c^*_{N(Me)_4Br} + c^*_{NiBr_2}$ is shown. c^* is given in the aquamolality scale, moles salt/55.5 moles of D_2O. We have $c^*_{N(Me)_4Br} = c^*_{NiBr_2}$. It will be seen that $1/T_1$ is almost proportional to the concentration c^*; merely at the lowest concentrations a feeble deviation from linearity appears, which is shown in more detail in Figure 1b. The slope of the relaxation rate, $d(1/T_1)/dc^*$ decreases as c^* decreases. We have to show that $1/T_1$ given in Fig. 1 really is an intermolecular relaxation rate caused by magnetic dipole-dipole interaction with the Ni^{2+} ion. For this purpose we consider Fig. 2, which gives the relaxation rate of $N(CH_3)_4Br$ in a solution with $MgBr_2$ in D_2O, again with $c^* = c^*_{N(Me)_4Br} + c^*_{MgBr_2}$ and $c^*_{N(Me)_4Br} = c^*_{MgBr_2}$. The limiting value of $1/T_1(N(Me)_4Br)$ for $c^* \to 0$ with $c^*_{MgBr_2} = 0$ is $0.097\ s^{-1}$; so according to Fig. 2 at $c^* = 1$ m we have $1/T_1 = 0.13\ s^{-1}$. The molecular motion effects of Ni^{2+} and Mg^{2+} are about equal, so inspection of Figs. 1 and 2 tells us that the intramolecular contribution to $1/T_1(N(CH_3)_4Br)$ is in fact negligible. This means that we can apply (3) and (4) with the data given in Figure 1. In the present system the correlation time τ is the electron spin relaxation time; it is of the order 10^{-12} s [6, 7]. The relaxation is caused by the spin-orbit interaction of the unpaired electrons in the presence of hydration water, and we have no indication that τ varies appreciably in the concentration range of interest to us. Furthermore, in the low concentration range, where deviations of $1/T_1$ from linearity occur, it is allowed to neglect the difference between the molality and molarity scales; we have set $c^* = c$ and performed the evaluation according to (4);

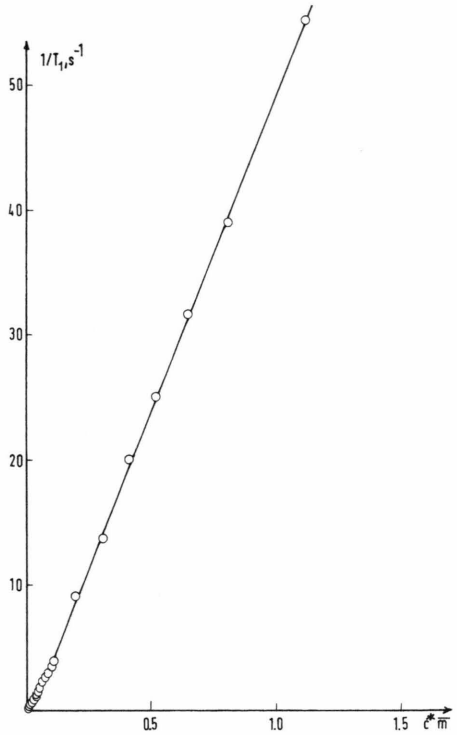

a)

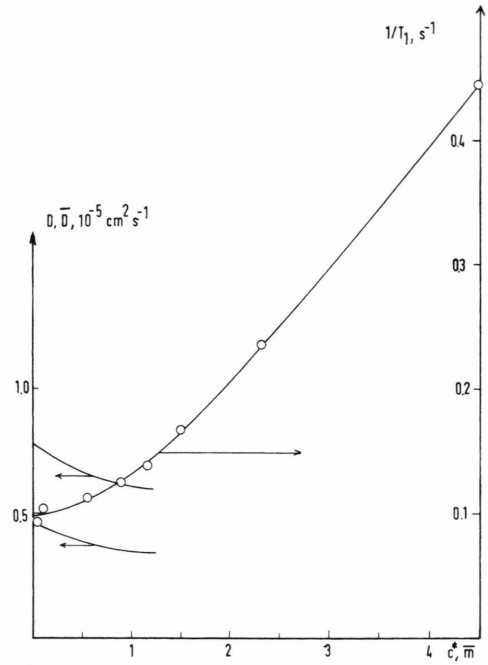

Fig. 2. Proton relaxation rate of the system $(CH_3)_4NBr/MgBr_2/D_2O$ as a function of the total cation concentration with $c^*_{NMe_4^+} = c^*_{Mg^{++}}$, $T = 25\,^\circ C$. Left-hand part: lower curve self-diffusion coefficient of Mg^{++} in $H_2O + MgCl_2$, upper curve mean self-diffusion coefficient $1/2(D_{Mg^{++}} + D_{NMe_4^+})$. $T = 25\,^\circ C$.

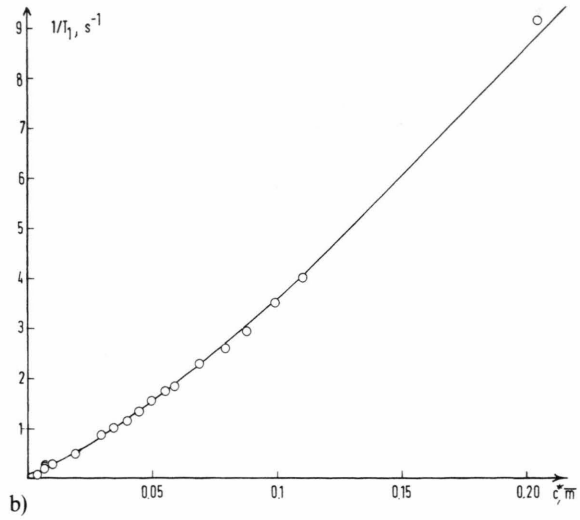

b)

Fig. 1. a) Proton magnetic relaxation rate $1/T_1$ of the system $(CH_3)_4NBr/NiBr_2/D_2O$ as a function of the total cation concentration with $c^*_{NMe_4^+} = c^*_{Ni^{++}}$. $\nu_0 = 90$ MHz, $T = 25\,^\circ C$, $\bar{m}$ = aquamolality scale. – b) Details of a) at low solute concentration.

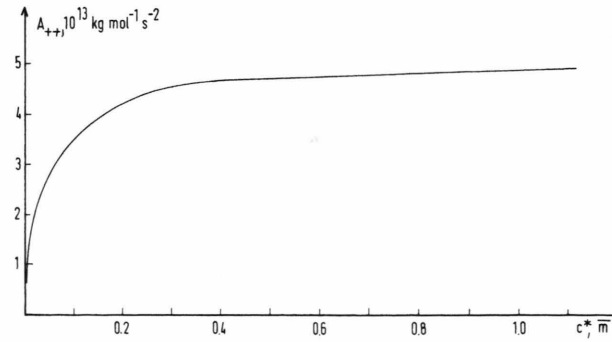

Fig. 3. Association (A-)parameter referring to the $NMe_4^+ - Ni^{++}$ pair distribution function as function of the total cation concentration in the system $NMe_4Br/NiBr_2/D_2O$. $T = 25\,^\circ C$.

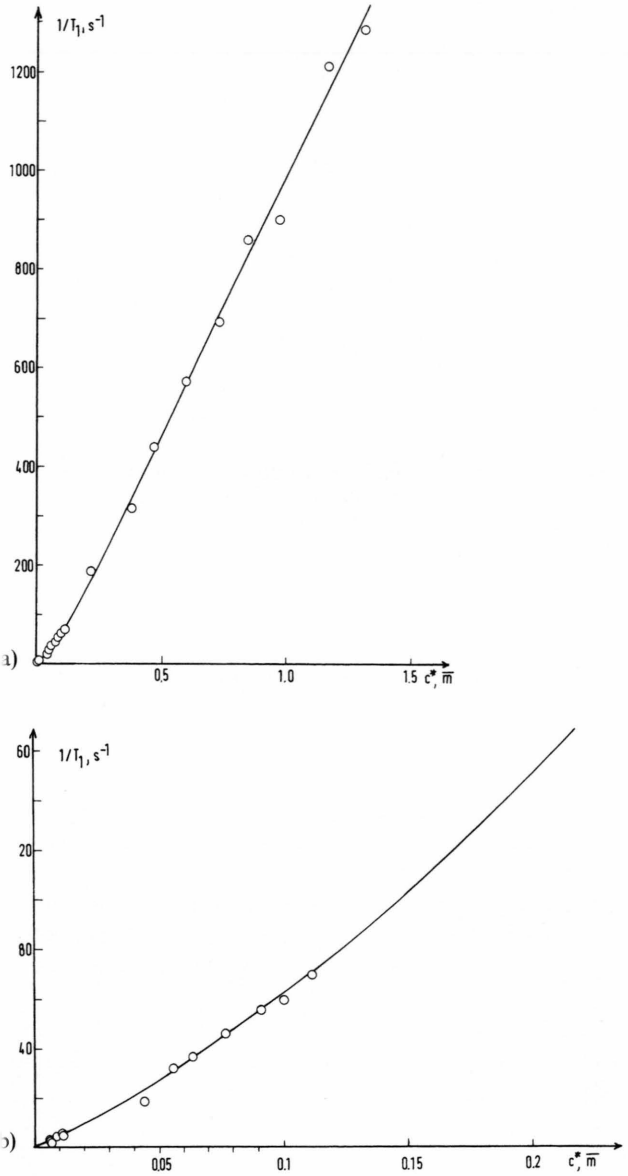

Fig. 4. a) Proton relaxation rate of the system $(CH_3)_4NBr/MnBr_2/D_2O$ as a function of the total cation concentration with $c^*_{NMe_4^+} = c^*_{Mn^{++}}$. $\nu_0 = 90$ MHz, $T = 25\,^\circ C$. – b) Details of a) at low solute concentration.

the result is shown in Figure 3. It will be seen that we have in fact a decrease of the A-parameter, that is $dn^*_{++}/dc^* > 0$ (de-association) is confirmed as expected from (5).

In Figs. 4 and 5 we show the corresponding results for the system $N(CH_3)_4Br + MnBr_2 + D_2O$. The only difference is that for Mn^{2+} the electron spin relaxation

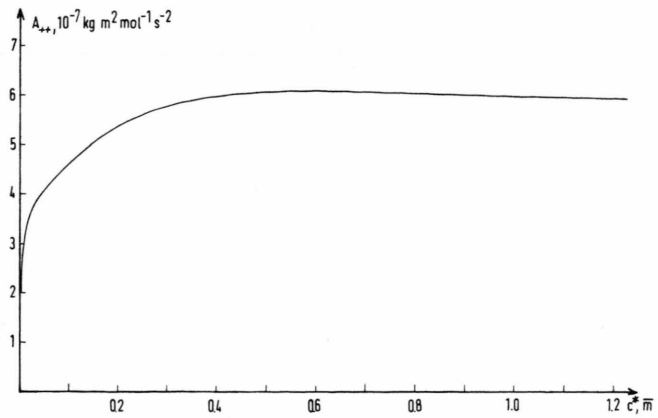

Fig. 5. A-parameter referring to the $NMe_4^+ - Mn^{++}$ pair distribution function as a function of the total cation concentration in the system $NMe_4Br/MnBr_2/D_2O$. $T = 25\,^\circ C$.

time is ca. 10^{-8} s [6]. Thus it is longer than the correlation time of the $^1H-Mn^{2+}$ magnetic dipole-dipole interaction which is of the order of 10^{-11} s. We set $\tau = a^2/3\,\bar{D}$ [12] where a is the closest distance of approach between the cationic protons and the centre of the Mn^{2+} ion. $\bar{D}$ is the mean self-diffusion coefficient of the cations, an approximate value is given as the upper curve on the left-hand side of Fig. 2 [13–15]. The lower curve is the self-diffusion coefficient of Mg^{2+} in the system $MgCl_2 + H_2O$ [16]. For all cases where the interaction partner is not member of an ionic solvation sphere we have no indication that this approximation of τ is inapplicable, see also [1–4]. Furthermore, in all cases studied our association statements based on the A-parameter are confirmed by the observation of positive velocity correlations [1, 17–21].

Figure 5 again demonstrates that A decreases with decreasing concentration, thus, as expected, cation-cation repulsion causes de-association when the solution becomes more diluted. Further details will be given in the discussion.

3.2 Cation-Anion Correlations

Figure 6 shows the proton-magnetic relaxation rates of nickel acetate $Ni(OOCCH_3)_2$, ($NiAc_2$), dissolved in D_2O. As will be seen from Fig. 6, at about $c^* \approx 0.8$ m we have fairly strong deviation from linearity; it is due to comples formation

$$Ni^{2+} + Ac^- \overset{K_1}{\leftrightarrow} NiAc^+,$$
$$NiAc^+ + Ac^- \overset{K_2}{\leftrightarrow} Ni(Ac)_2$$

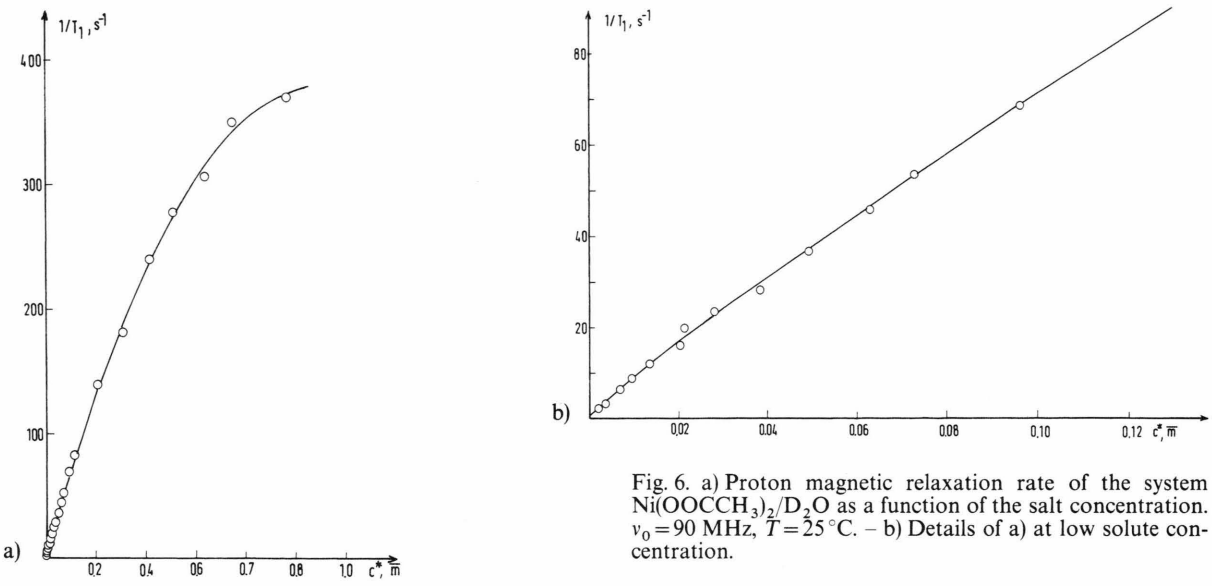

Fig. 6. a) Proton magnetic relaxation rate of the system $Ni(OOCCH_3)_2/D_2O$ as a function of the salt concentration. $\nu_0 = 90$ MHz, $T = 25\,^\circ C$. – b) Details of a) at low solute concentration.

with $\log K_1 = 0.58$ and $\log K_2 = 0.67$ [22]. Computation of relative species distribution yields the result that at $c^* = 0.1$ we have ca. 9 percent $NiAc^+$ and 9 percent $Ni(Ac)_2$, both contributions decreasing rapidly as we go towards $c^* \to 0$. Figure 7 gives the corresponding A-parameter according to (4), where again we have assumed $\tau \approx$ const (τ the electron spin relaxation time). We see that, in contrast to the features of Figs. 3 and 5, now the A-parameter increases with decreasing salt concentration, we have cation-anion association [1].

General linearity of $1/T_1$ is better fulfilled for the solution of $Mn(Ac)_2$ in D_2O, as is seen in Figure 8. Thus, here complex formation is absent or at least not detectable by our method. The slight curvature at low concentrations is magnified in Figure 8b. We calculated the A-parameter with the same mean self-diffusion coefficient as used for the system $N(Me)_4Br + MnBr_2 + D_2O$, the $c^* \to 0$ limiting ionic conductivities for $N(Me)_4^+$ and CH_3COO^- are almost the same [23]. In the present system the A-parameter (see Fig. 9) is almost constant in the range $0.5 < c^* < 1.2$ m̄, then it increases by a factor of ≈ 4 as c^* decreases to $c^* = 0.001$ m̄. This differs from the behaviour of the $NiAc_2$ solution. Here the increase of A is smeared over a wide concentration range which certainly is due to the complex formation existing for the $NiAc_2$ system.

Note that at higher concentrations, $c^* \approx 1$ m̄, where the A-parameter varies little, it is 6–7 times larger for the anion-cation interaction than for the cation-cation interaction.

3.3 Diamagnetic Systems, Relaxation by Quadrupole Interaction

So far our proof that cation-anion association and cation-cation de-association, respectively, exist at high dilution was based on a particular kind of interaction, the magnetic dipole-dipole interaction between the proton and the unpaired electrons. The latter particles possess a certain distribution in space, moreover they exert contact interaction with nuclei [5, 6, 9]. To make sure that our association results are not special properties of the dipole-dipole interaction we

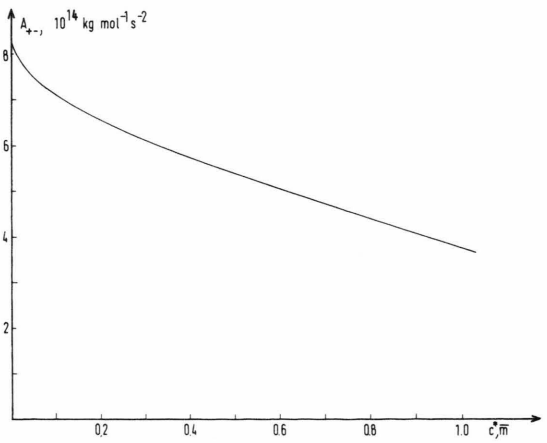

Fig. 7. A-parameter referring to the $CH_3COO^- - Ni^{++}$ pair distribution function in the system $Ni(OOCCH_3)_2/D_2O$. $T = 25\,^\circ C$.

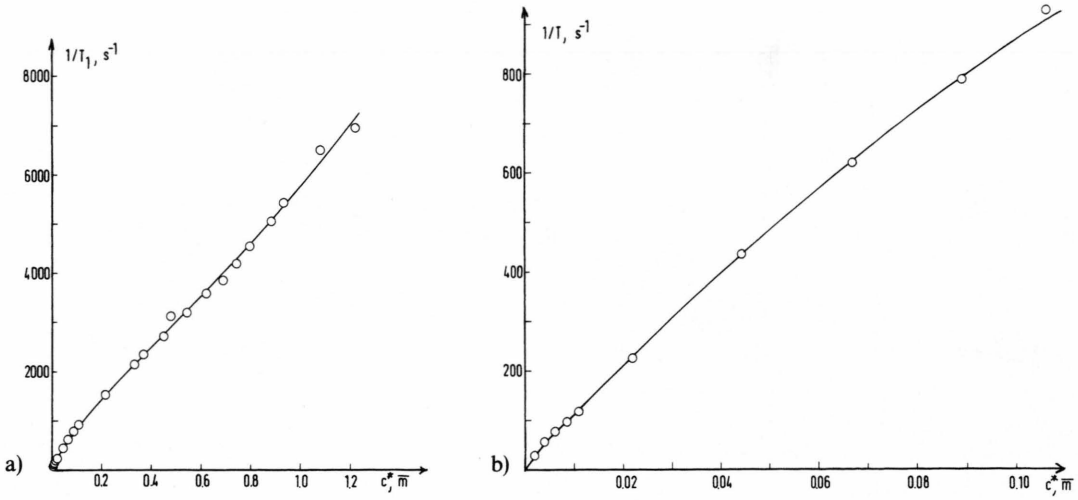

Fig. 8. a) Proton magnetic relaxation rate of the system $Mn(OOCCH_3)_2/D_2O$ as a function of the salt concentration. $\nu_0 = 90$ MHz, $T = 25\,^\circ C$. – b) Details of a) at low concentration.

confirm them by studying systems where the nuclear quadrupole-electric field gradient interaction is the cause of magnetic relaxation. As already mentioned, however, it is not possible to separate cation-anion effects from cation-cation effects, yet, in a certain way in contrast to the dipole-dipole situation, we consider it to be of interest to study the combined effect of cations and anions. In Fig. 10 we show $1/T_1$ results for ^{35}Cl in a number of electrolyte solutions (LiCl, RbCl, HCl, CsCl and $MgCl_2$). These data confirm our previous finding [24, 25] that $1/T_1$ at low concentrations is proportional to $\sqrt{c^*}$, see Fig. 11 which already indicates on a qualitative basis that there is anion-cation association as $c^* \to 0$ (compare Figs. 6a and 8a). Within experimental error our present results, when extrapolated to concentrations $c^* \geq 1$ m, are consistent with our previous measurements at higher concentrations [26]. The order of the relaxation rate increases with c^*, i.e. $CsCl > RbCl \approx LiCl$, is the same as previously found at higher concentrations ($H^{35}Cl$ and $Mg^{35}Cl_2$ have not been measured before). In [25] we studied mostly the magnetic relaxations of cationic nuclei, i.e. $^7Li^+$, $^{23}Na^+$, $^{87}Rb^+$; some $^{81}Br^-$ results were also given. Having found the square root concentration dependence for all these systems it is the more surprising that an increase of the slope $d(1/T_1)/dc^*$ as $c^* \to 0$ was not detectable for the $^{25}Mg^{++}$ relaxation in the solution of $MgCl_2$, as will be seen from Figure 12. We have included experimental values of Struis and Leyte in Fig. 12 [27]; these data confirm the correctness of our measurements.

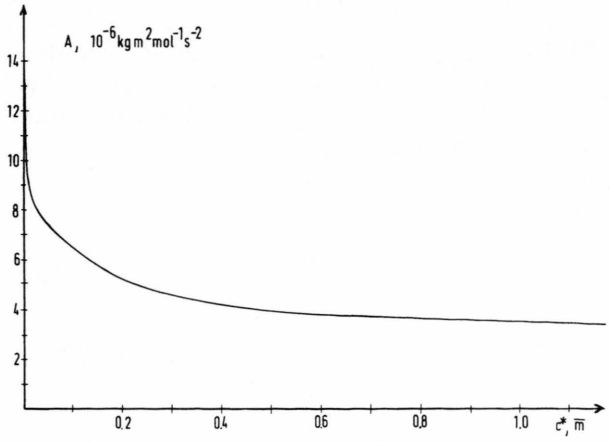

Fig. 9. *A*-parameter referring to the $CH_3COO^- - Mn^{++}$ pair distribution function in the system $Mn(OOCCH_3)_2/D_2O$, $T = 25\,^\circ C$.

In analogy to (1), the relaxation rate caused by quadrupole interaction essentially is the mean squared nuclear quadrupole interaction with the local electric field gradient, to which the total surrounding contributes. It follows that the path to our proof of ion-ion association for $c^* \to 0$ will be more complicated.

As a first consequence, it is not possible to remove the ion-solvent contribution by isotopic substitution techniques. Thus we have

$$1/T_1 = (1/T_1)^{Cl^- - H_2O} + (1/T_1)^{ion\text{-}ion}. \qquad (7)$$

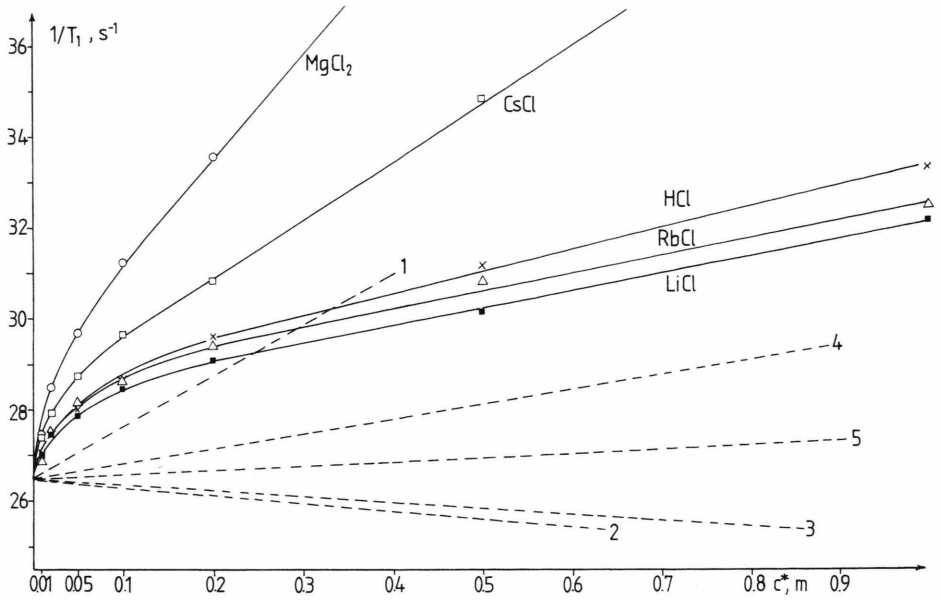

Fig. 10. $^{35}Cl^-$ magnetic relaxation rates in a number of aqueous solutions as a function of the salt concentration (in molality scale, m). The dashed straight lines represent approximate solvent contribution to the relaxation rates. 1: $MgCl_2$, 2: CsCl, 3: RbCl, 4: LiCl, 5: HCl. $T = 25\,^{\circ}C$, $\nu_0 = 23.39$ MHz, water $= H_2O$.

The ion-ion contribution is the object of our study (association indicator), and the ion-solvent contribution has to be calculated. For our purpose it is sufficient to write for the ion-solvent contribution [25]

$$(1/T_1)^{Cl-H_2O} = K_{is} n_h \tau_w , \tag{8}$$

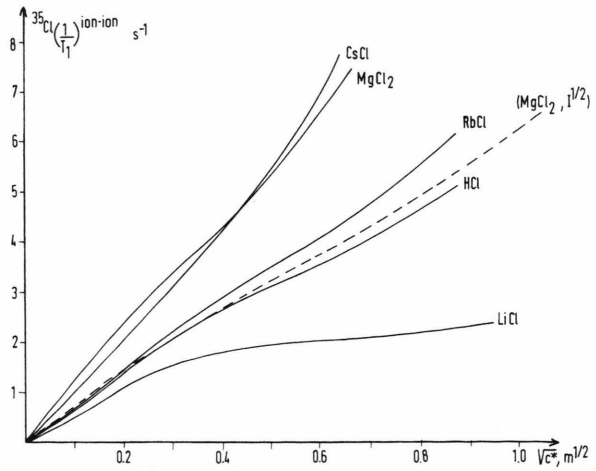

Fig. 11. Ion-ion contribution to the $^{35}Cl^-$ relaxation rates shown in Fig. 10 as a function of concentration. The dashed curve for $MgCl_2$ is obtained if the numbers on the abscissa represent ionic strengths.

where K_{is} is a constant, n_h is the effective number of water molecules around the Cl^- ion not being effected by geometrical correlations with the approaching counter ion, and τ_w is the reorientation time of these water molecules, τ_w is a function of the salt concentration; let τ_0 be the reorientation time of pure water, then we set [25]

$$\tau_w = \tau_0 \varkappa(c^*) \frac{^h(1/T_1)_{c^*}}{^h(1/T_1)_0} . \tag{9}$$

$^h(1/T_1)$ is the hydrogen nucleus magnetic relaxation rate (^1H or ^2H), the meaning of the subscript "0" is again pure water, $\varkappa(c^*)$ transforms from the mean solution reorientation time to the local reorientation time at the relaxing ion. As we did previously [25], we use the approximation

$$\varkappa = \varkappa_0 + \frac{1-\varkappa_0}{6} c^* \quad \text{for } 0 < c^* < 6\ \bar{m} . \tag{10}$$

For Cl^- we have $\varkappa_0 \approx 1$ [28], for Cs^+, to be used below, $\varkappa_0 = 0.5$ [28]. In Fig. 10 we have included $(1/T_1)^{Cl^- - H_2O}$ according to (8)–(10) as dashed straight lines. Having thus given a scheme to extract the ion-ion contribution from the total relaxation rate, this term has to be analysed in order to verify that the quadrupole mech-

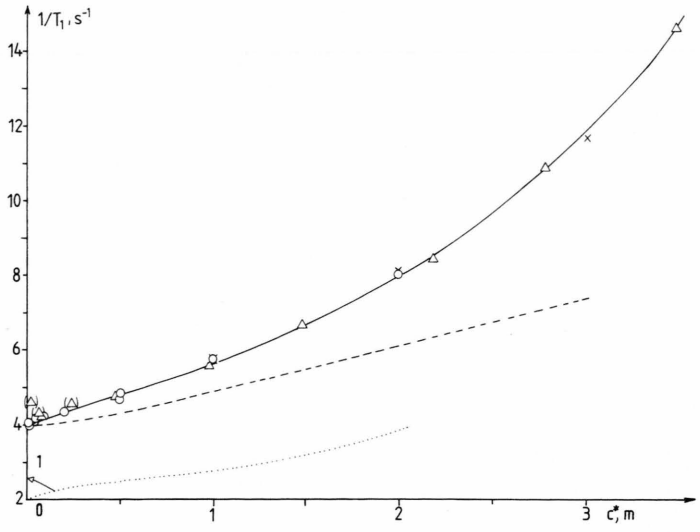

Fig. 12. $^{25}Mg^{++}$ magnetic relaxation rates of solution of $MgCl_2$ in H_2O as functions of the concentration c^* (molality scale) o: this work, Δ: after lit. [14] (Δ) to our oppinion unprecise results, ×: after lit [33]. The dashed curve represents a possible solvent contribution, the dotted curve the corresponding ion-ion contribution; $T = 25\,^{\circ}C$, $\nu_0 = 18.36$ MHz.

anism as well shows strong electrolyte ion-ion association at high dilution. As the electric field gradient has many contributions, the corresponding expression is a little more complicated.

$(1/T_1)^{\text{ion-ion}}$ is given by a relation of the form (for more details see [25])

$$\left(\frac{1}{T_1}\right)^{\text{ion-ion}} = \frac{c^*}{\bar{D}}\left[K_{i1}\frac{1}{a^4}\int_a^{a'}\left(\frac{a}{r}\right)^6 f_{iw}(r)\hat{g}_{+-}(r)r^2\,dr + K_{i2}\frac{1}{a'^4}\int_{a'}^{\infty}\left(\frac{a'}{r}\right)^6 f_{ii}(r)(g_{+-}(r)+g_{--}(r))r^2\,dr\right], \quad (11)$$

where K_{i1} and K_{i2} are constants, a is the closest distance of approach between anions and cations, $f_{iw}(r)$ describes the effect of those water molecules in the first coordination sphere of the reference ion (here Cl^-) which are geometrically correlated with the approaching counter ion (here the cation), at a distance a' such correlation have disappeared, $\hat{g}_{+-}(r)$ is a cation-anion pair correlation function also involving the occurrence probability of proper water-counter ion configuration [25]. In the second term on the right-hand side of (11) we find contributions from both kinds of ions. But the motions of cations and anions are correlated. The counter ions (the cations here) are screened by the like ions, and vice versa. The screening is the more effective the higher the concentration. Thus, the screening function goes to zero for larger r values, and the range of decay is roughly given by the Debye length. The important point is that the integrals of (11) also contain the function $(a/r)^6 g(r) r^2$ occuring in (2) and (5) and yielding the basic purpose of this work, however in a somewhat more involved form.

In Fig. 11 $(1/T_1)^{\text{ion-ion}}$ as the difference between the full and dashed curves in Fig. 10 has been plotted as a function of $\sqrt{c^*}$. The linear $\sqrt{c^*}$ dependence at small c^* values has already been mentioned, the order of the strength of the ion-ion relaxation effect has now changed:

$$Li^+ < Na^+ \approx H^+ < Rb^+ < Cs^+ \approx Mg^{2+}.$$

The influence of LiCl and $MgCl_2$ has decreased strongly as compared with the curves of Fig. 10, which means that for these solutions the increase of the water reorientation time with increasing salt concentration plays an important role. Mg^{2+} and Li^+ are "structure forming" cations, Cs^+ and Rb^+ are "structure breaking" ions; here the appreciable ion-ion contribution is certainly due to water-cation correlations expressed by the function $f_{iw}(r)$ in the first integral of (11). If we plot $(1/T_1)^{\text{ion-ion}}$ versus the square root of the ionic strength, then in the order just given Mg^{2+} is even placed close to H^+ (see Figure 11).

In Fig. 12 we have included a dashed curve which shows a possible behaviour of $(1/T_1)^{Mg^{2+}-H_2O}$. It is drawn in such a form that $\varkappa$ according to (10) is not a linear function; rather τ_w stays constant for a small concentration range around $c^* \approx 0$. In this way the lowest curve in Fig. 12 results as $(1/T_1)^{\text{ion-ion}}$ which should also yield an increasing A-parameter as given for the ^{35}Cl systems in Fig. 13 and thus demonstrating high-dilution anion-cation association. The A-curves

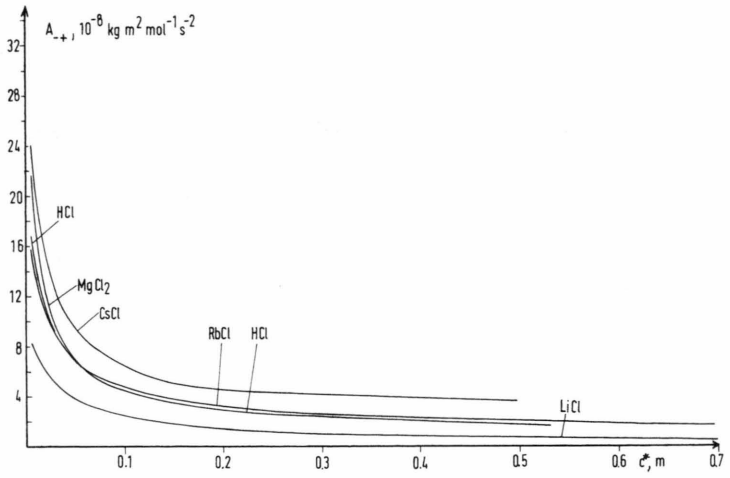

Fig. 13. The ion-ion A-parameter of the system the relaxation data of which are shown in Fig. 10, derived from the curves given in Figure 11.

in Fig. 13 were obtained by the use of the left-hand part of (4) with (13), where according to the purpose of this paper we have set $(1/T_1)_{\text{inter}} = (1/T_1)^{\text{ion-ion}}$ according to (11).

The self-diffusion data to be used to get A have been taken from [15, 25, 29]. As we go from $c^* = 0.5$ to $c^* = 0.005$ m, the A-parameter increases by a factor of $\approx 7, 11, 9, 7$, and 12 for CsCl, Mg, Cl_2, HCl, RbCl, and LiCl, respectively. We learn from these data that the increase of the A-parameter due to quadrupole relaxation of ^{35}Cl is stronger than that observed for protons which relax by dipole-dipole interaction (Figs. 7 and 9). In our previous work [25] we found similar A-values, although the results there were not extended to such high dilutions as achieved here ($A(0.1)/A(0.5) \approx 2.3-5.5$).

In Fig. 14 we show ^{133}Cs relaxation rates in various electrolyte solutions. It will be seen that in most cases $1/T_1$ is smaller than the extrapolation value of $c^* \to 0$. In fact, we have observed previously that at higher concentration, $c^* \geq 1$ m̄, for some ^{133}Cs halide solutions (except CsF) $1/T_1 < 1/T_1\,(c^* \to 0)$ [30, 31]. This is the first case observed that the mean squared electric field gradient at the centre of an ion decreases when, started with the isolated ion, $c^* = 0$, the concentration of the salt considered is increased, that is, the number of other ions which should be the sources of additional field gradients, becomes larger. Yet, is the proof of cation-anion association still feasible? The answer is yes, as will be shown below.

It should be remarked in passing that Rb^+ has not this property of relaxation loss as the concentration increases starting from $c^* = 0$ [25]. We have performed measurements in the solvents D_2O and H_2O in order to make sure that the relaxation mechanism really is the quadrupole interaction. Indeed, the H_2O results lie below the D_2O curves, which shows that the shorter correlation time makes the difference of the $1/T_1$ values and not the larger magnetic moments of ^{1}H. The $1/T_1\,(c^* \to 0)$ extrapolation value in H_2O is slightly higher than expected (86%) [32]. In Fig. 14 we have again drawn the dashed straigth lines which give the expected concentration dependence of τ_w for the

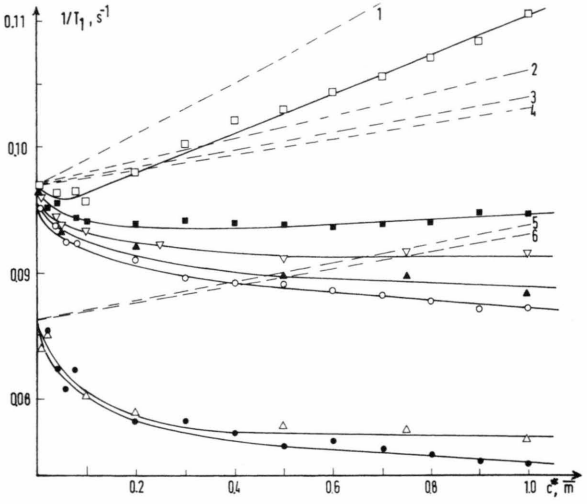

Fig. 14. $^{133}Cs^+$ relaxation rates of various cesium salt solution in D_2O (upper set of curves) and in H_2O (lower set of curves). Dashed straight lines represent approximations of the uncorrelated solvent contribution to the $^{133}Cs^+$ relaxation rates. 1, 2, 3, 4: CsF, CsCl, CsBr and CsI, respectively in D_2O, 5 and 6: CsCl and CsBr in H_2O. $T = 25\,^\circ$C, $\nu_0 = 39.35$ MHz. ○, ● CsBr, △, ▲ CsCl, ▽ CsI, ■ $CsNO_3$, □ CsF.

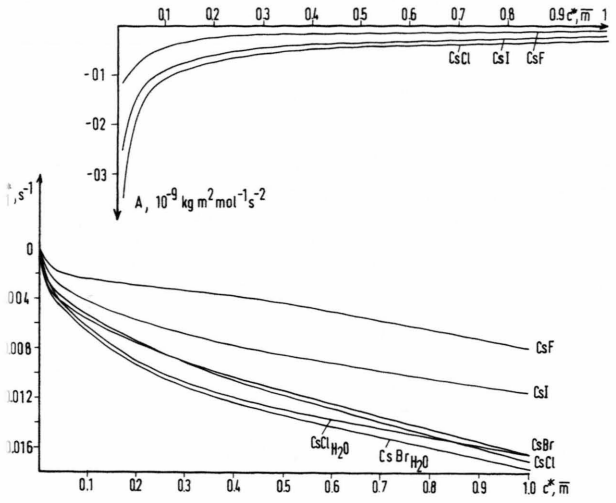

Fig. 15. Ion-ion + correlated solvent contribution to the relaxation rate of $^{133}Cs^+$ in H_2O and D_2O solutions. – *Inset*: A-parameters for three of the solutions considered here.

substraction of the ion-solvent contribution as described above (see (8)–(10)). It will be seen that all variations of reorientation times τ_w are not negligible, they demonstrate the transition from the local water motion around the structure breaking ion Cs^+ to the mean structure breaking effect in the total solution at $c^* = 6$ m̄ (see (10)). Since F^- is a structure former the exception is again the case of CsF.

In Fig. 15 $1/T_1^*$, the difference between the fully drawn and dashed curves in Fig. 14, is depicted, it shows the "convex" concentration dependence typical for cation-anion association at high dilution, but the sign is reversed. The conclusion is that the decrease of the ^{133}Cs relaxation rate as c^* increases certainly is not an effect of the uncorrelated water molecules, it must be due to the electric field gradient of the water molecules, the configuration of which is correlated with the position of the colliding anions. The CsCl and CsBr curves for the solutions in H_2O and D_2O are slightly different, which is a consequence of the fact that we do not know exactly the correct $c^* \to 0$ extrapolation value in H_2O.

The water-anion correlation appears twice in the formulas given above. (I) in (8) n_h decreases as c^* increases. (II) the function $f_{iw}(r)$ in (11) assumes values differing from unity. In previous work [25] the relation

$$f_{iw}(r) = \left(1 + \frac{9mr^3}{2er_0^4} O(\Theta, \vartheta)\right)^2$$

was derived. m is the electric dipole moment of the water molecule, the meaning of the symbols Θ, ϑ, and r_0 may be seen from Figure 16. The function $O(\Theta, \vartheta)$ has values between -2 and $+2$, for the present anion-cation configuration $9mr^3/2er_0^4 \approx 1$. Taking a collision distance $r = 4$ Å we have $\Theta = 50°$ and $f_{iw}(r) = 0$ for $\vartheta = -60°$, as shown in Figure 16. If we accept this value $f_{iw} = 0$, then the total effect of the anion on the ^{133}Cs relaxation is a decrease of the effective number of uncorrelated water molecules n_h as given (by (8)) by ca. 15 percent in the range $0 < c^* < 1$ m̄. F^- is more strongly hydrated, Θ is smaller and $f_{iw}(r) > 0$ results, so that the field gradient quenching effect of the water molecules is weaker.

Thus, the curves indicated as "ion-ion" in Fig. 15 are not the direct ionic effect, rather they are the particular effect of the water molecules produced by the presence of the approaching anions which in turn undergo association with the cation Cs^+ at high dilution. Indeed one can derive an A-parameter from the curves Fig. 15 according to the prescription

$$A = (1/T_1)^{\text{ion-ion}} \cdot \frac{\bar{D}}{c}.$$

Of course now A is negative, and it is the A-parameter indirectly caused by the associating cation-anion pairs via the dimple formed by the water molecules in the encounter configuration. The results are shown in the inset of Figure 15.

4. Discussion

In this discussion we compare the observed behaviour of the A-parameter with the prediction accord-

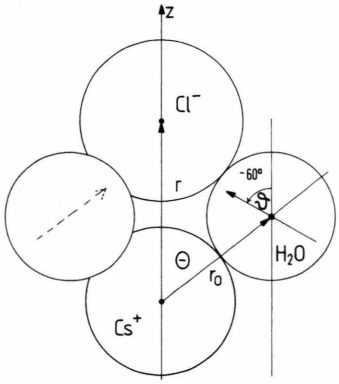

Fig. 16. Cs^+–Cl^- encounter configuration causing the negative A-parameter shown in Figure 15.

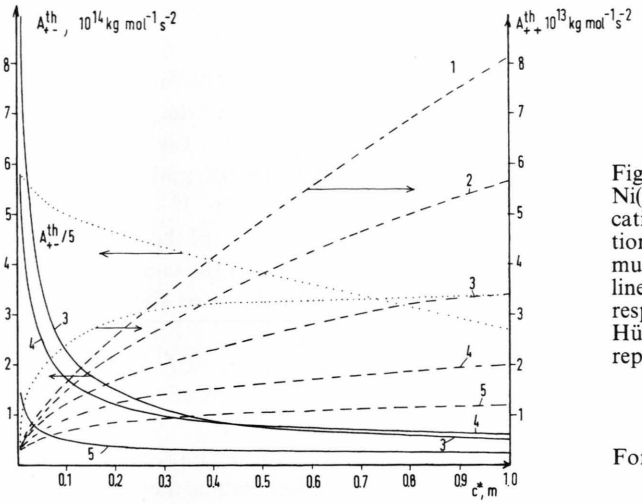

Fig. 17. Theoretical A-parameters, A^{th}_{+j}, for the solutions of $Ni(OOCCH_3)_2$ and $N(Me)_4Br-NiBr_2$, calculated from the cation-anion and cation-cation Debye-Hückel pair distribution function for a 2-1 electrolyte. The data given contain a multiplicative factor as given in the text. Solid and dashed lines represent cation-anion and cation-cation A-parameters, respectively. The numbers at the curves are the Debye-Hückel b-parameters in Ångström units. The dotted curves represent the quantities

$$\frac{A^{th}_{+j}(c^*=0.005)_b}{A_{+j}(c^*=0.005)} A_{+j}(c^*), \quad j=+,-.$$

For further details see text.

ing to the Debye-Hückel theory. We define a Debye-Hückel A-parameter by the relation

$$A^{DH}_{+j} = 4\pi \int_b^\infty g_{+j}(r) \frac{dr}{r^4}, \qquad j=-,+$$

with $g_{+j}(r) = e^{-w_{+j}/kT}$, (12)

where $w_{+j} = \frac{q_+ q_j}{\varepsilon r} \frac{e^{-\varkappa(r-b)}}{1+\varkappa b}$, $\qquad j=-,+$

is the potential of mean force between the ions, q_+ and $q_- > 0$ being the charges of the ions,

$$\varkappa^2 = \frac{4\pi e^2 (c'_+ z_+^2 + c'_- z_-^2)}{\varepsilon k T},$$

$$z_i = |q_i|/e, \quad i=+,-.$$

ε is the dielectric constant and b is the closest distance of approach between the ions in the sense of the Debye-Hückel theory. c'_+, c'_- are the number densities of cations and anions, respectively. In (2) and (5) $a=b$, however, the relation for the correlation time

$$\tau = \frac{a^2}{3\bar{D}}, \tag{13}$$

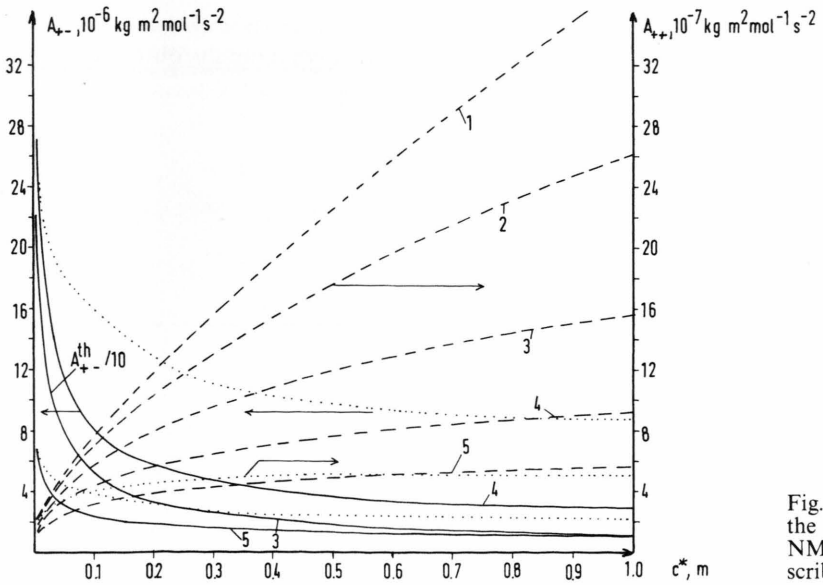

Fig. 18. Theoretical A-parameter A^{th}_{+j} for the solution of $Mn(OOCCH_3)_2$ and $NMe_4Br-MnBr_2$. All other details as described for Figure 17.

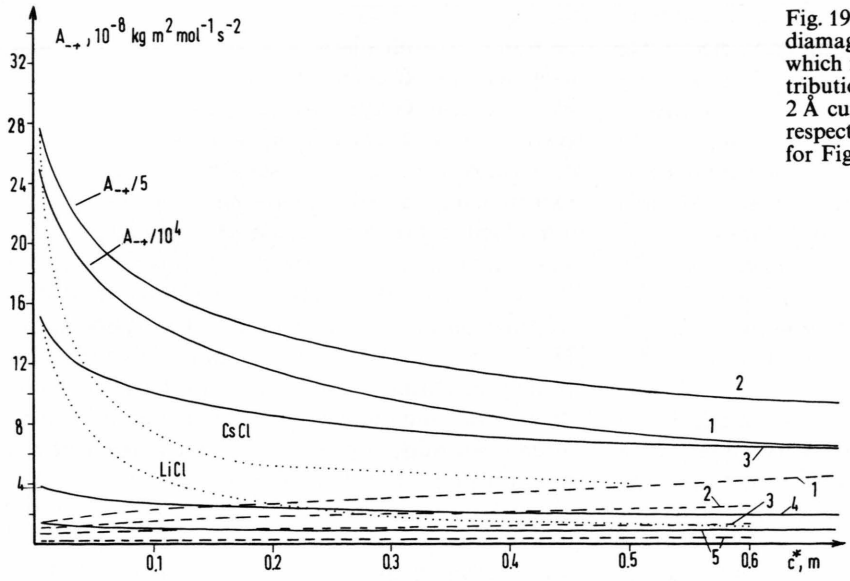

Fig. 19. Theoretical A-parameters for the diamagnetic solutions investigated here which now involve the Debye-Hückel distribution for 1-1 electrolytes. The 1 Å and 2 Å curve represent $A_{-+}/10^4$ and $A_{-+}/5$, respectively. All other details as described for Figure 17.

involving the closest distance of approach a is an approximation [20], and thus the precise equality $a=b$ is not required.

The results for A_{+j}^{DH} are given in Figs. 17–19 in the form:

$$\mathrm{Ni}^{++}\colon A_{+j}^{\mathrm{th}} = 4.97\cdot 10^{-4}\,\mathrm{kg\,m^3\,mol^{-1}\,s^{-2}}\cdot A_{+j}^{\mathrm{DH}},\quad j=+,-.$$

The factor of proportionality is $a^6 K$ according to (3a) divided by $\tau = 10^{-12}$ s.

$$\mathrm{Mn}^{++}\colon A_{+j}^{\mathrm{th}} = 2.30\cdot 10^{-23}\,\mathrm{kg\,m^5\,mol^{-1}\,s^{-2}}\cdot A_{+j}^{\mathrm{DH}},\quad j=+,-.$$

The factor of proportionality is $a^6 K$ according to (3a) multiplied by $a^2/3$ according to (13), and $a=3.65$ Å, chosen so as to bring A_{+j}^{th} in the proper range.

$$\mathrm{Cl}^{-}\colon A_{+-}^{\mathrm{th}} = 1.76\cdot 10^{-25}\,\mathrm{kg\,m^5\,mol^{-1}\,s^{-2}}\cdot A_{+-}^{\mathrm{DH}},$$

where in (11) the two constants K_{i1} and K_{i2} have been contracted to the factor of proportionality [25]

$$\frac{6\pi}{5}\,\frac{2I+3}{I^2(2I-1)}\left[\frac{eQ}{\hbar}(1-\gamma_\infty)P\right]^2\frac{1}{4\pi}\,\frac{e^2}{9}\,\frac{a^2}{3},$$

and we have set $a=4$ Å. (Q = electric quadrupole moment, γ_∞ = Sternheimer factor, P = polarization factor). These theoretical A-parameters A_{+j}^{th} can directly be compared with the experimental ones A_{+j} given in Figs. 3, 5, 7, 9, and 13. For the paramagnetic solutions the A_{+j}^{th}'s belonging to $b=1$ Å and $b=2$ Å have comparatively very large values between $4\cdot 10^{15}$ and $5\cdot 10^{21}$ kg mol^{-1} s^{-2} for Ni^{++} and between $2\cdot 10^{-4}$ and $2\cdot 10^{2}$ kg m^2 mol^{-1} s^{-2} for Mn^{++}.

Comparison of the curves given in Figs. 3, 5, 7, 9, and 13 with those presented in Figs. 17–19 shows that the theoretical and experimental A-parameters are indeed of the same order of magnitude. To obtain a more detailed comparison we have included the experimental A-parameters in Figs. 17–19 in such a manner that by multiplication of $A_{+j}(c^*)$ by a factor $A_{+j}^{\mathrm{th}}(0.005)/A_{+j}(0.005)\equiv\alpha$ we obtain equal A-parameters at $c^*=0.005$ m.

The quantities

$$\alpha A_{+j}(c^*) \equiv \frac{A_{+j}^{\mathrm{th}}(0.005)}{A_{+j}(0.005)}\,A_{+j}(c^*),\quad j=+,-$$

are drawn as dotted curves in Figures 17–19. Turning first to the Ni^{++} results, Fig. 17, we see that the $\alpha A_{++}(c^*)$ curve is closest to the theoretical one for $b=3$ Å. In order to get coincidence at $c^*=0.005$ we would have to compute A_{++}^{th} with $\tau=0.63$ ps instead of $\tau=1$ ps. In the range $0.01<c^*<0.5$, $\alpha\cdot A_{++}(c^*)$ differs markedly from A_{++}^{th} for $b=3$ Å. For A_{+-}^{th} with $b=4$ Å, $\tau=1.4$ ps yields coincidence $A_{+-}=A_{+-}^{\mathrm{th}}$ at $c^*=0.005$ m, however at higher concentrations the curvature of $A_{+-}(c^*)$ is much weaker that that of A_{+-}^{th}. It is almost not necessary to remark that at higher concentrations $c^*\gtrsim 0.01$ m the Debye-Hückel pair

distribution function is no longer exactly valid, so from both sides, the NMR relaxation and electrolyte solution theory, the comparisons given here can only be of qualitative nature. Next we consider the Mn^{++} results, Figure 18. To get coincidence of $A_{++}(0.005)$ and $A^{th}_{++}(0.005)$ we have to set $a=4.1$ Å with $b=1$ Å, or $a=5.2$ Å with $b=5$ Å. The experimental $\alpha \cdot A_{+-}(c^*)$ curve essentially crosses the A^{th}_{++} curves for $b=2, 3, 4$ Å as c^* increases. For A_{+-} we have shown two $\alpha \cdot A_{+-}(c^*)$ curves which give $A_{+-}(0.005)=A^{th}_{+-}(0.005)$: for $b=5$ Å, $a=4.65$ Å is required, for $b=4$ Å, $a=2.32$ Å has to be used. Again, the almost equality of a and b should not be overvalued.

Attention should also be paid to this reminder when we now turn to the diamagnetic systems, Fig. 9, where the evaluation contains many approximations. For the LiCl solution we get agreement $A_{+-}(0.005)=A^{th}_{+-}(0.005)$ when we set $a=2.9$ Å for the computation of A^{th}_{+-} with $b=3$ Å, for the CsCl solution the corresponding figures yielding coincidence at $c^*=0.005$ m̄ are $a=1.7$ Å with $b=2$ Å, so interpolation yields the results $a=b=3.15$ Å and $a=b=2.2$ Å for LiCl and CsCl solution, respectively. It is a well known fact that the $Cl^- - Cs^+$ approach is closer than that between Cl^- and Li^+ [30, 31]. The other systems, solutions of HCl, RbCl and $MgCl_2$, yield numerical values between these extreme ones. It will be seen from Fig. 19 that the curvatures of the experimental $A_{+-}(c^*)$ curves are much stronger than those of the theoretical ones. Note that we have compared $A(c^*)$ with A^{th}_{+-}; however, we might have compared $A_{+-}(c^*)$ with $A^{th}_{+-}+A^{th}_{--}$. Since A^{th}_{--} is much smaller than A^{th}_{+-}, and the relaxation theory involves another averaging process, the central features of our conclusion are not altered by this simplification. Summarizing, we obtain the result that our observed ion-ion association and de-association effects at high dilution are in qualitative agreement with the predictions given by the electrostatic Debye-Hückel theory. However, close agreement between the closest distances of approach, the "experimental" a and "theoretical" b, should not be overvalued. Yet there is one aspect which gives a particular importance to our results. This is the fact that Pettitt and coworkers have claimed that in strong electrolyte solutions there is $Cl^- - Cl^-$ association, [34–37] see also [38]. Thus one could argue that the strongly increasing A-parameters we have observed are due to anion-anion association, not to anion-cation association. However, the close agreement between a and b, where b stems from the Debye-Hückel theory, may be taken as an indication that our observed strongly increasing A-parameter is indeed due to cation-anion association. Consequently, if there were anion-anion association as well, then the A-parameter in our systems should be about twice as large as predicted by the Debye-Hückel pair distribution functions, which however has not been observed. Exception is the CsCl solution, here a certain degree of microheterogeneity has been postulated so that part of the strong increase of A_{+-} is in fact due to close $Cl^- - Cl^-$ neighbourhood [31].

Acknowledgement

We wish to thank Dipl. Phys. Ralf Haselmeier for his calculation of the Debye-Hückel A-parameters. One of the authors (X. M.) is grateful to the "Alexander von Humboldt-Stiftung" for financial support.

[1] K. J. Müller and H. G. Hertz, Chemica Scripta **29,** 277 (1989).
[2] U. Wandler and H. G. Hertz, Z. Phys. Chem. **178,** 217 (1992).
[3] M. Holz, R. Grunder, A. Sacco, and A. Meleleo, J. Chem. Soc. Faraday Trans. **89,** 1215 (1993).
[4] M. Holz and K. J. Patil, Ber. Bunsenges. Phys. Chem. **95,** 107 (1991).
[5] A. Abragam, Principles of Nuclear Magnetic Resonance Clarendon, Oxford 1961.
[6] N. Bloembergen and L. O. Morgan, J. Chem. Phys. **34,** 842 (1961).
[7] F. Hirata, H. L. Friedman, M. Holz, and H. G. Hertz, J. Chem. Phys. **73,** 6031 (1980).
[8] M. Holz, H. L. Friedman, and B. L. Tembe, J. Magnetic Resonance **47,** 454 (1982).
[9] See also L. Banci, I. Bertini, and C. Luchinat, Nuclear and Electron Relaxation. Verlag Chemie, Weinheim 1991.
[10] M. Holz, N. W. Lutz, F. Blumenthal, and H. G. Hertz, J. Soln. Chem. **9,** 381 (1980).
[11] H. G. Hertz and M. Holz, J. Magn. Reson. **63,** 64 (1985).
[12] See e.g. H. G. Hertz in Molecular Motions in Liquids ed. J. Lascombe p. 337, Reidel Publ. Comp., Dordrecht 1974.
[13] H. G. Hertz, B. Lindman, and V. Siepe, Ber. Bunsenges. Phys. Chem. **73,** 542 (1969).
[14] L. A. Woolf and H. Weingärtner, Faraday Symp. Chem. Soc. **17,** 41 (1982).
[15] R. Mills and V. M. M. Lobo, Self-diffusion in Electrolyter Solutions, Elsevier, Amsterdam 1989.
[16] K. R. Harris, H. G. Hertz, and R. Mills, J. Chim. Phys. **75,** 391 (1978).
[17] H. G. Hertz, K. R. Harris, R. Mills, and L. A. Woolf, Ber. Bunsenges. Phys. Chem. **71,** 664 (1977).
[18] H. G. Hertz and R. Mills, J. Phys. Chem. **82,** 952 (1978).
[19] H. G. Hertz and G. Leiter, Z. Phys. Chem. Neue Folge **133,** 45 (1982).

[20] S. Prabhakar and H. Weingärtner, Z. Phys. Chem. N.F. **137,** 1 (1983).
[21] H. Weingärtner, Ber. Bunsenges. Phys. Chem. **94,** 358 (1990).
[22] Stability Constants of Metal-Ion Complexes, eds. J. Bjerrum, G. Schwarzenbach, and L. G. Sillén, The Chemical Soc., London 1957.
[23] R. A. Robinson and R. H. Stokes, Electrolyte Solutions, Butterworth, London 1970.
[24] A. Sacco, M. Holz, and H. G. Hertz, J. Magn. Resonance **65,** 82 (1985).
[25] H. G. Hertz, M. Holz, and A. Sacco, Chemica Scripta **29,** 291 (1989).
[26] M. Holz and H. Weingärtner, J. Magn. Resonance **27,** 153 (1977).
[27] R. P. W. I. Struis, I. de Bleijser, and I. C. Leyte, J. Phys. Chem. **93,** 7932 (1989).
[28] L. Endom, H. G. Hertz, B. Thül, and M. D. Zeidler, Ber. Bunsenges. Phys. Chem. **71,** 1008 (1967).
[29] H. G. Hertz, A. Maitra, R. Mills, and H. Weingärtner, J. Chim. Phys. **78,** 67 (1981).
[30] H. G. Hertz, M. Holz, G. Keller, H. Versmold, and C. Yoon, Ber. Bunsenges. Phys. Chem. **78,** 493 (1974).
[31] H. G. Hertz and R. Mazitov, Ber. Bunsenges. Phys. Chem. **85,** 1103 (1981).
[32] A. Sacco, H. Weingärtner, B. M. Braun, and M. Holz, J. Chem. Soc. Faraday Trans. **90,** 849 (1994).
[33] M. Holz, S. Günther, O. Lutz, A. Nolle, and P. G. Schrade, Z. Naturforsch. **34a,** 944 (1979).
[34] B. M. Pettitt and R. J. Rossky, J. Chem. Phys. **84,** 5836 (1986).
[35] L. X. Dang and B. M. Pettitt, J. Chem. Phys. **86,** 6560 (1987).
[36] L. X. Dang and B. M. Pettitt, J. Am. Chem. Soc. **109,** 5531 (1987).
[37] L. X. Dang and B. M. Pettitt, J. Phys. Chem. **94,** 4303 (1990).
[38] H. Xu and H. L. Friedman, J. Soln. Chem. **19,** 1155 (1990).